Molecular Interactions between Proteins and Synthetic Membrane Polymer Films

Frederic Pincet,† Eric Perez,† and Georges Belfort*

Howard P. Isermann Department of Chemical Engineering, Rensselaer Polytechnic Institute, Troy, New York 12180-3590

Received August 27, 1993. In Final Form: December 5, 1994®

To help understand the effects of protein adsorption on membrane filtration performance, we have measured the molecular interactions between cellulose acetate films and two proteins with different properties (ribonuclease A and human serum albumin) with a surface force apparatus. Comparison of forces between two protein layers with those between a protein layer and a cellulose acetate (CA) film shows that, at high pH, both proteins retained their native conformation on interacting with the CA film while at the isoelectric point (pI) or below the tertiary structure of proteins was disturbed. These measurements provide the first molecular evidence that disruption of protein tertiary structure could be responsible for the reduced permeation flows observed during membrane filtration of protein solutions and suggest that operating at high pH values away from the pI of proteins will reduce such fouling.

Introduction

During the filtration of protein-containing solutions with pressure-driven membrane processes, the protein molecules often adsorb onto and into the membranes. Besides this adsorption process, exposure to fluid shear stresses can also denature the protein molecules rendering desorption difficult if not impossible. Adsorption of protein molecules in the membrane pores will affect the mean pore size and pore-size distribution available for the flow and, hence, the permeation and retention characteristics of the membrane.[1]

Much work has been reported on membrane filtration with solutions containing macromolecules such as proteins [bovine serum albumin (BSA), ovalbumin and lactoglobulins], poly(vinyl alcohol), polyethylene glycol, dextrans, and others. The decline of flux with time or total integrated volume permeated was initially explained as membrane compaction. However, it soon became clear that different rates of flux decline occurred with different solutions under similar experimental conditions.

Several phenomena have been proposed to explain this. They include (1) protein adsorption, aggregation, and gel formation, due to the effect of pH and ionic strength on the solute–solute and solute–membrane interactions,[2-13] and (2) reduced driving force caused by the effect of the osmotic pressure due to the buildup of macromolecules at the solution–membrane interface.[14-18] One of the most studied model protein systems for understanding membrane polarization and fouling has been BSA solutions. For example, fluxes are higher when the pH is away from the isoelectric point (pI) of the protein,[2,4,5,10,19] when little salt is present,[10] and when the surface chemistry of the membrane is hydrophilic.[19]

In order to help understand these effects, direct measurements of the intermolecular forces between selected model proteins, such as ribonuclease A (RNase A) and human serum albumin (HSA), and a widely used synthetic membrane material, cellulose acetate (CA), have been measured. After describing the procedures used with the surface force apparatus, details are presented on the proteins and the cellulose acetate material. The properties of CA films and those of two adsorbed HSA layers are first characterized by force measurements. Then, results consisting of the direct measurements of the intermolecular forces between HSA and CA, and RNase A and CA are presented.

* Corresponding author.

† Laboratoire de Physique Statistique, Ecole Normale Superieure, 24 rue Lhomond, 75005 Paris, France.

® Abstract published in *Advance ACS Abstracts,* February 15, 1995.

(1) Belfort, G.; Pimbley, J. M.; Greiner A.; Chung, K-Y. Diagnosis of membrane fouling using a rotating annular filter. 1. Cell culture media. *J. Membr. Sci.* **1993**, *77*, 1–22.

(2) Fane, A. G.; Fell, C. J.; Suzuki, A. The effect of pH and ionic environment on the ultrafiltration of protein solutions with retentive membranes *J. Membr. Sci.* **1983**, *16*, 195–210.

(3) Mattiasson, E. Role of macromolecular adsorption in fouling of ultrafiltration membranes *J. Membr. Sci.* **1983**, *16*, 23–36.

(4) Nystrom, M., Laatikainen, M., Turku, M.; Jarvinen, P. Resistance to fouling accomplished by modification on ultrafiltration membranes *Prog. Colloid Polym. Sci.* **1990**, *52*, 321–329.

(5) McDonogh, R. M.; Bauser, H.; Stroh, N.; Chmiel, H. Concentration polarization and adsorption effects in cross-flow ultrafiltration of proteins *Desalination* **1990**, *79*, 217–231.

(6) Robertson, B. C.; Zydney, A. L. Protein adsorption in asymmetric ultrafiltration membranes with highly constricted pores *J. Colloid Interface Sci.* **1990**, *134* (2), 563–575.

(7) Meireles, M.; Aimar, P.; Sanchez, V. Albumin denaturation during ultrafiltration: effects of operating conditions and consequences on membrane fouling *Biotechnol. Bioengr.* **1991**, *38*, 528–534.

(8) Nabetani, H.; Nakajima, M.; Watanabe, A.; Nokao, S.; Kimura, S. Effects of osmotic pressure and adsorption on ultrafiltration of ovalbumin *AIChE J.* **1990**, *36* (6), 907–915.

(9) Blatt, W. F.; Dravid, A.; Michaels, A. S.; Nelson, L. *Membrane Science & Technology;* Flinn, J. E., Ed.; Industrial Biological Waste Treatment Processes; Plenum Press: New York, 1970.

(10) Fane, A. G.; Fell, J. D.; Waters, A. G. Ultrafiltration of protein solutions through partially permeable membranes-the effect of adsorption and solution environment *J. Membr. Sci.* **1983**, *16*, 211–224.

(11) Nakao, S.; Nomura, T.; Kimura, S.; Characteristics of macromolecular gel layer formed on ultrafiltration tubular membrane *AIChE J.* **1979**, *25*, 615–622.

(12) Nakao, S.; Kimura, S. Analysis of solutes rejection in ultrafiltration *J. Chem. Engr. Jpn 14* (1), **1981**, 32–37.

(13) Tirmizi, N. P., Study of UF of macromoleculars solutions Ph.D. thesis, Department of Chemical Engineering, RPI, Troy, NY, 1990.

(14) Goldsmith, R. L. Macromolecular ultrafiltration with microporous membranes *Ind. Eng. Chem. Fundam.* **1971**, *10*, 113–120.

(15) Leung, W. F.; Probstein, R. F. Low polarization in laminar ultrafiltration of macromolecular solutions *Ind. Eng. Chem. Fundam.* **1979**, *18* (3), 274–278.

(16) Viker, V. L.; Colton, C. K.; Smith, K. The osmotic pressure of concentrated protein solutions: effects of concentration and pH in saline solutions of bovine serum albumins *J. Colloid Interface Sci.* **1981**, *79* (2), 548–566.

(17) Jonsson, G. Boundary layer of phenomena during ultrafiltration of dextran and whey protein solutions *Desalination* **1984**, *51*, 61–77.

(18) Wijmans, J. G.; Nakao, S.; Smolders, C. A. Flux limitation in ultrafiltration: osmotic pressure model and gel-layer model *J. Membr. Sci.* **1984**, *20*, 115–124.

(19) Hannemaaijer, J. H.; Robertsen, T.; van der Boomgaard, Th.; Olieman, C.; Both, P.; Schmidt, D. G. Characterization of cleaned and fouled ultrafiltration membranes *Desalination* **1988**, *68*, 93–108.

0743-7463/95/2411-1229$09.00/0

Materials and Methods

Surface Force Apparatus (SFA). The technique involves the direct measurements of the intermolecular forces between two separate layers; one, an adsorbed protein layer, and the other, a film of cellulose acetate or adsorbed protein. Each layer is deposited onto a smooth mica half-cylinder. The forces are obtained as a function of separation distance, which is measured with an interferometry technique.[20,21] It is the same method as that used to elucidate the intermolecular forces and conformation of adsorbed molecules between mica surfaces covered with surfactant,[22-24] polymers,[25-30] lipid mono- and bilayers,[31-35] proteins,[36-43] and glycolipids.[44] The mica surfaces were immersed in aqueous electrolyte solution within a small Teflon bath. A 10^{-2} M KCl solution was used in all experiments unless otherwise stated. During each experiment, the KCl concentration and the pH value were kept constant. The pH value was, however, varied from one experiment to the next. A 10^{-2} M KCl concentration corresponds to a 3 nm Debye decay length. We therefore considered 3 nm as a reference for characterizing the measured forces. If the observed decay length (λ) was much larger than 3 nm, then long-range steric interactions were likely. Overlapping denatured proteins were mainly responsible for these steric forces, while electrostatic interactions were shorter-ranged. Alternately, if λ was close to 3 nm, then electrostatic forces dominated. At pH 2 and 10^{-2} M KCl concentration, the electrolyte concentration was 2×10^{-2} M. This corresponded to a Debye decay length of 2.2 nm rather than the 3 nm. The room temperature was controlled at 20 ± 0.5 °C, and all the solutions were in thermal equilibrium with room temperature for at least 6 h before injection in the Teflon bath.

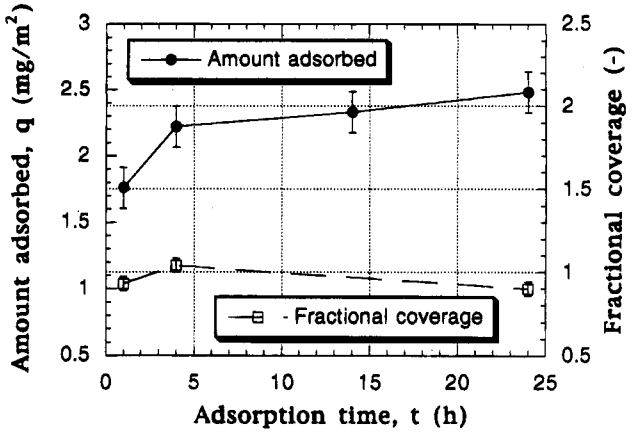

Figure 1. Amount of hydrated RNase A adsorbed and fractional surface coverage on mica as a function of time. The solution contained a RNase A concentration of 0.1 mg/mL in 10^{-2} M KCl, pH 5, and at 20 ± 0.5 °C.

Proteins. Two proteins with different properties were chosen: ribonuclease A (RNase A) and human serum albumin (HSA). RNase A is a small stable protein while HSA is large and relatively easy to denature. RNase A was purchased from Pharmacia Biotech. (RNase A I "A"). The dimensions of a hydrated folded RNase A molecule are 2.8 × 3.4 × 4.4 nm and its molecular weight is 13 690 Da. Since the pH was the main variable used in this study, it is important to note that the pI of RNase A is 9.2. Previously unpublished adsorption measurements by Cheng Sheng Lee of our laboratory between hydrated RNase A and mica at a solution concentration of 0.1 mg/mL in 10^{-2} M KCl, pH 5, and at 20 ± 0.5 °C are summarized in Figure 1.[45] The method used to obtain these results was based on a measurement of the variation of refractive index in the SFA between the two mica surfaces as a function of adsorption time and separation distance together with the appropriate calibration curves. The total estimated error in determining the adsorbed amounts was ±10%. Although the amount adsorbed increases with time, the fractional coverage appears to remain constant at about 100% at and after 1 h adsorption. The reason for this, as confirmed by the SFA measurements,[37] is that the RNase A molecules change their orientation within a *monolayer coverage* on the surface with time from side on to end on, thus allowing more protein to adsorb and resulting in an increased protein density at the mica interface with time.

HSA was purchased from Sigma (HSA #3782). Hydrated HSA is heart-shaped, i.e. it can be approximated to a solid equilateral triangle with sides of about 8.6 nm, a base length of about 8.1 nm, and an average depth of 3.6 nm.[46] Its molecular weight is 68 500 Da and its pI is 4.8. Another difference between the

(20) Israelachvili, J. N.; Adams, G. E. Measurements of forces between two mica surfaces in aqueous electrolyte solutions in the range 1–100 nm *J. Chem. Soc. Faraday Trans. 1* **1978**, *74*, 975–1001.
(21) Israelachvili, J. N. Measurements of forces between surfaces immersed in aqueous electrolyte solutions *Faraday Discuss. Chem. Soc.* **1978**, *65*, 20–24.
(22) Israelachvili, J. N.; Pashley, R. M. The hydrophobic interaction is long-range, decaying exponentially with distance *Nature* **1982**, *300*, 341–343.
(23) Israelachvili, J. N.; Pashley, R. M. Measurement of the hydrophobic interactions between two hydrophobic surfaces in aqueous solution *J. Coll Intf. Sci* **1984**, *98*, 500–514.
(24) Pashley, R. M.; McGuiggan, P. M.; Ninham, B. W.; Evans, D. F. Attractive forces between uncharged hydrophobic surfaces: direct measurements in aqueous solution *Science 229*, 1088–1089.
(25) Israelachvili, J. N.; Tirell, M.; Klein, J.; Almong, Y. Forces between two layers of adsorbed polystyrene immersed in cyclohexane below and above the θ temperature *Macromolecules* **1984**, *17*, 204–209.
(26) Klein, J. Forces between mica surfaces bearing layers of adsorbed polystyrene in cyclohexane Nature (London), **1980**, *288*, 248–250.
(27) Klein, J.; Luckham, P. F. Long-range attractive forces between two mica surfaces in an aqueous polymer solution Nature (London), **1984**, *308*, 836–837.
(28) Klein, J.; Luckham, P. F. Interactions between proteins and synthetic polypeptides adsorbed at solid-liquid interfaces *Colloid Surf.* **1984**, *10*, 65–76.
(29) Claesson, P.; Golander, C. Direct measurements of steric interactions between mica surfaces covered with electrostatically bound low molecular weight polyethylene oxide *J. Coll. Intf. Sci.* **1987**, *117*, 366–374.
(30) Klein, J. Long-ranged surface forces: The structure and dynamics of polymers at interfaces *Proc. Appl. Chem.* **1992**, *64*, 1577–1584.
(31) Marra, J. Controlled deposition of lipid monolayers and bilayers onto mica and direct force measurements between galactolipid layers in aqueous solutions *J. Coll. Intf. Sci.* **1985**, *107*, 446–458.
(32) Marra, J.; Israelachvili, J. N. Direct measurements of forces between phosphatidylcholine and phosphatidylethanolamine bilayers in aqueous electrolyte solutions *Biochemistry* **1985**, *24*, 4608.
(33) Chen, Y. L.; Helm, C. A.; Israelachvili, J. N. Measurements of the elastic properties of surfactant and lipid monolayers *Langmuir* **1991**, *7*, 2694–2699.
(34) Helm, C. A.; Knell, W.; Israelachvili, J. N. *Proc. Nat'l. Acad. Sci.* **1991**, *88*, 8169–8173.
(35) Leckband, D. E.; Israelachvili, J. N.; Schmitt, F. J.; Knell, W. Long-range attraction and molecular rearrangements in reactor-ligand interactions *Science* **1992**, *255*, 1419–1421.
(36) Perez, E.; Proust, J. Forces between mica surfaces covered with adsorbed mucin across aqueous solutions *J. Coll. Intf. Sci.* **1987**, *118*, 182–1991.
(37) Lee, C. S.; Belfort, G. Changing activity of ribonuclease A during adsorption: A molecular explanation *Proc. Nat'l. Acad. Sci.* **1989**, *86*, 8392–8396.
(38) Belfort, G.; Lee, C. S. Attractive and repulsive interactions between and within adsorbed ribonuclease A layers *Proc. Nat'l. Acad. Sci.* **1991**, *88*, 9146–9150.
(39) Blomberg, E.; Claesson, P. M.; Gölander, C. Adsorbed layers of human serum albumin investigated by the surface force technique *J. Disp. Sci., Technol. 12*, **1991**, (2) 179–200.
(40) Malmsten, M.; Blomberg, E.; Claesson, P.; Carlsted, I.; Ljusegren, I. Mucin layers on hydrophobic surfaces, studies with ellipsometry and surface force measurements *J. Coll. Intf. Sci.* **1992**, *151*, 579–590.
(41) Fitzpatrick, H.; Luckham, P. F.; Eriksen, S.; Hammond, K. Bovine serum albumin adsorption to mica surfaces *Colloid & Surfaces* **1992**, *64*, 43–49.
(42) Kekicheff, P.; Ducker, W. A.; Ninham, B. W.; Pileni, M. P. Multilayer adsorption of cytochrome C on mica around isoelectric pH *Langmuir* **1990**, *6*, 1704–1708.
(43) Leckband, D.; Israelachvili, J. N. Molecular basis of protein function as determined by direct force measurements *Microb. Technol.* **1993**, *15*, 450–459.
(44) Luckham, P.; Wood, J.; Swart, R. The surface properties of gangliosides II. Direct measurements of the interaction between bilayers deposited onto mica surfaces *J. Coll. Intf. Sci.* **1993**, *156*, 173–183.
(45) Lee, C. S. Direct measurements of intermolecular forces between ribonuclease A layers sorbed onto mica. Thesis submitted in partial fulfillment of Ph.D., Department of Chemical Engineering, Rensselaer Polytechnic Institute, Troy, NY, 1988.
(46) He, X. M.; Carter, D. C. Atomic structure and chemistry of human serum albumin *Nature* **1992**, *358*, 209–215.

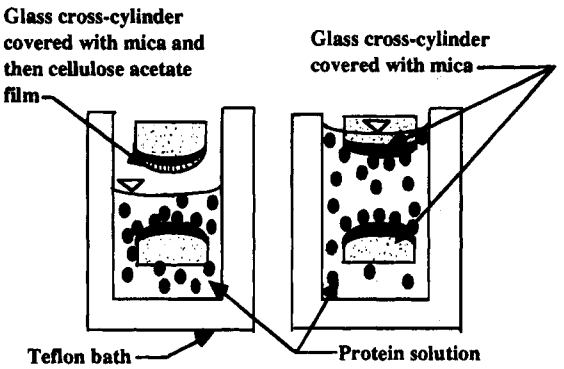

Figure 2. Schematic showing the two cross-mica cylinders for (a) one surface covered with the protein solution and for (b) both surfaces covered with the protein. In part a this ensured that protein was not adsorbed onto the upper surface.

properties of these two proteins is their adiabatic compressibility values in water at 25 °C. This parameter is qualitatively used to distinguish between rigid ($\beta_s = 1.12 \times 10^{-11}$ N/m^2 for RNase A) and flexible ($\beta_s = 10.5 \times 10^{-11}$ N/m^2 for bovine serum albumin) proteins.[47] Blomberg et al. (Figure 1 of ref 39) have published adsorption isotherm data for HSA. From this figure of Blomberg et al. and the data in Figure 1 shown here, it is clear that, for solution protein concentrations of 5×10^{-3} mg/mL used in this study, adsorbed monolayers of the same dimension as the native proteins lying side on are expected.

Three types of experiments were conducted. In the first type of experiment, one mica surface was covered with cellulose acetate (CA) and the other was left bare. In the second type of experiment, both mica surfaces were covered by adsorbed HSA. A similar experiment for RNase A has been reported in the literature.[37,38] In the third type of experiment, one mica surface was covered with CA and the other covered with protein. The first step of the adsorption procedure was to inject the protein solution (always 5×10^{-3} mg/mL) into the SFA, the protein being in its native state (Figure 2). Since the adsorption rate depended on the particular protein, the time to reach saturation was protein dependent. For each protein, however, the adsorption time was kept constant for all experiments. It has already been shown that, with RNase A, an adsorption time of about 20 h provided full and dense coverage of the mica sheets.[37,38] For HSA, the problem was more complicated since it tended to aggregate. We conducted several experiments with HSA adsorbed onto both surfaces. The results showed that if HSA adsorbed for 3 h or more, a strong repulsive force appeared when the mica surfaces were far apart. This suggested that aggregation of HSA occurred between the mica sheets. We therefore chose to restrict adsorption to 2 h and considered that this time was sufficient for monolayer coverage of HSA. After adsorption was completed, the protein solution was flushed three times with 10^{-2} M KCl solution. Then, the final protein-free KCl solution (10^{-2} M) was injected into the SFA. The pH of these KCl solutions was always kept the same as the pH of the protein solution. For each protein, experiments were conducted at three different pH values: above, below, and at the pI. Note that, though mica is a negatively charged material under the conditions used here, proteins, because they are amphoteric and contain hydrophobic patches, can adsorb even above their pI (i.e. when the net charge is negative).

Cellulose Acetate. As one of the most widely used synthetic membrane materials for pressure-driven membrane processes, cellulose acetate (CA) is an appropriate choice for this study. Its chemical structure results in a relatively hydrophilic surface (Figure 3). For this study, cellulose acetate with a degree of substitution of 2.5 (40.3% acetyl content) was used. It was prepared by dipping the mica directly into a pure acetone solution of cellulose acetate (10^{-4} wt %) as per Riley et al.[48] In order to reduce the thickness of the adsorbed film, nitrogen gas was

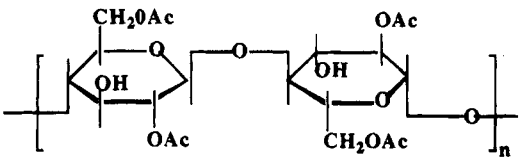

Cellulose acetate

[Ac = -COCH$_3$]

Figure 3. Chemical structure of cellulose acetate (CA).

pressured onto the newly formed CA film on the mica immediately after dipping. The local smoothness of the film was satisfactory for SFA measurements since, by changing somewhat the position of the contact surface, the thickness of the film did not vary significantly. Unfortunately, the reproducibility of this approach (with respect to thickness) was relatively poor; the film thickness could vary from 20 to 200 nm This large variation in thickness made interpolation of the distance measurements difficult. However, since the refractive index of CA (1.4 ± 0.1, 5 measurements) was close to that of water, we could delineate the results with a three-layer model (mica–CA/water–mica). Several properties of CA membranes were relevant for this work. First, under most conditions, the surface charge was negative due to the presence of disassociated carboxyl groups. At pH values lower than 4.5, the surface potential can switch to a positive value.[49] Vos et al.[50] measured the hydrolysis rate of cellulose acetate (39.8% acetyl content) at different temperatures (23–95 °C) as a function of pH (2.2–10). These rates were at a minimum at the pI (around 4.5). Second, CA films can be hydrolyzed to cellulose at high pH values. At pH values lower than 9, the hydrolysis rate was lower than 10^{-6} s^{-1}.[50] For this range of pH (2–9), the films were not significantly hydrolyzed during the experiment. However, some measurements were conducted at pH 11. For these cases, the hydrolysis process must be accounted for.

Results

Forces between a Cellulose Acetate (CA) Film and Mica. Compression of CA films resulted in compaction of the membrane pore structure. The membrane decompressed slowly and needed several hours to return to its original thickness. This, in turn, resulted in a hysteresis effect in the normalized force–distance curves and complicated the measurements. Because of membrane compaction, the force measurements during compression did not show the real interactions between the materials being studied. Thus, only force measurements during decompression were used. These measurements were highly reproducible. To handle this problem, we chose to compress each membrane down to a constant minimum thickness for all the runs in a given experiment so that the minimum distance to the mica was always the same (at normalized forces, >10 mN/m). Then, all the decompression curves could be superimposed. Here, only the decompression curves will be shown.

The interactions between CA and mica have been conducted at three different pH values, 2, 5, and 11. The results are given in Figure 4. The curves are very similar, and for the purpose of comparison with the forces between proteins and CA films, they can be considered identical at all pH values. Thus, the membrane behaved like a smooth solid wall. Besides the wall-like steric force, hardly any other forces were observed except for very weak electrostatic forces at long distances (>2 nm) that were possibly due to the low charge density on the CA film. The

(47) Gekko, K.; Hasegawa, Y. Compressibility–structure relationship of globular proteins *Biochemistry* **1986**, *25*, 6563–6571.

(48) Riley, R. L.; Londsdale, H. K.; Lyons, C. R.; Merten, U. Preparation of ultrathin reverse osmosis membranes and attainment of theoretical salt rejection *J. Appl. Polym. Sci.* **1967**, *11*, 2143–2158.

(49) Heyde, M. E.; Peters, C. R.; Anderson, J. E. Factors influencing reverse osmosis rejection of inorganic solutes from aqueous solution *J. Coll. Intf. Sci.* **1975**, *50*, 467–487.

(50) Vos, K. D.; Burris, Jr., F. O.; Riley, R. L. Kinetic study of the hydrolysis of cellulose acetate in the pH range of 2–10 *J. Appl. Polym. Sci.* **1966**, *10*, 825–832.

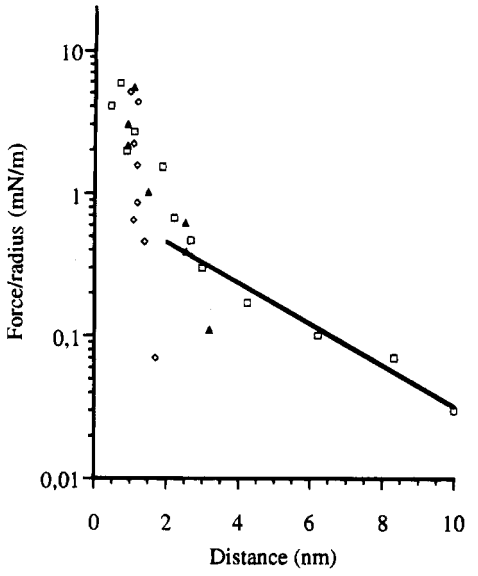

Figure 4. Normalized force versus separation distance between a deposited film of cellulose acetate (on mica) and mica in 10^{-2} M KCl solution at pH 2 (open diamonds), pH 5 (filled triangles), and pH 11 (open squares). The distance is that between the compressed cellulose acetate film and mica. The line is the theoretical Debye decay length (3 nm). Only decompression results are shown.

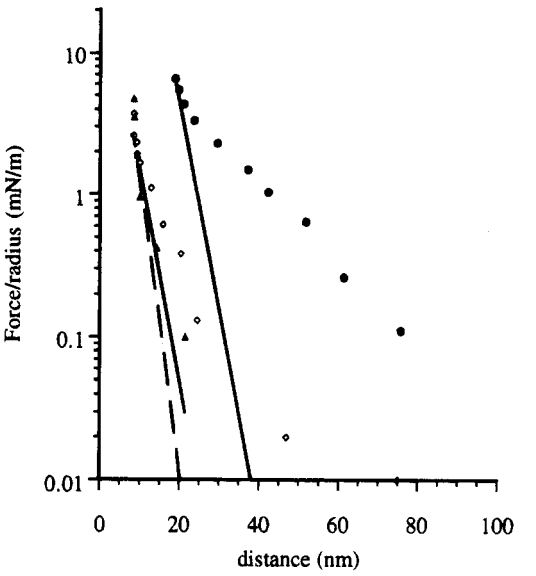

Figure 5. Normalized force versus separation distance between two adsorbed human serum albumin protein layers in a 10^{-2} M KCl solution at pH 2 (open diamonds), pH 4.8 (filled circles), and pH 9 (filled triangles). The lines are the theoretical Debye decay lengths (full line for pH 4.8 and 9, dashed line for pH 2). The difference between the measured slope and the Debye decay length is due to the steric interactions. The distance was that between the two mica surfaces. Compressions and decompressions were superimposable.

amplitude of these electrostatic forces was relatively small since, as will be observed later, forces about 10 times stronger than this were measured between proteins and the CA surface. Thus, besides the wall-like effect, there were no other observable steric interactions between CA and mica. The expected Debye decay length (3 nm) was observed at pH 11 for long distances in 10^{-2} M KCl. This suggests that the CA film was very smooth and few, if any, polymeric chains extended out from the surface. Thus, a dense CA membrane exhibited highly reproducible and simple behavior. Moreover, as already mentioned, membrane hydrolysis could have changed the nature of the surface at pH 11. These curves show that, at room temperature and on the time scale of the experiment (5–8 h), hydrolysis is not significant. To confirm this, a CA film was stored in a KCl solution at pH 11 for 20 h at 20 °C. This time is close to the time scale on which hydrolysis was relevant.[50] The normalized force–distance results before and after the 20 h exposure to high pH were markedly different (not shown). For the latter experiment, the decay length was 10 times higher than that measured in the former experiment. Clearly, strong electrostatic interactions appeared after a sufficient time, suggesting that the hydrolysis resulted in a partial degradation of the polymer. These broken polymer chains were able to extend into the solution. An alternative explanation could be delamination of the membrane. However, the results in Figure 4 show that for the conditions of the force experiments, the membrane is not significantly hydrolyzed even at pH 11.

Forces between Two HSA Adsorbed Layers. Three pH values were chosen: 2, 4.8, and 9. In all cases, the interactions were repulsive and approximately exponential. The thicknesses of the adsorbed HSA layers were obtained by measuring the distance between the two mica surfaces when the normalized force was 4–5 mN/m at low and high pH values (Figure 5 and Table 1). Steric interactions could also be estimated by subtracting the theoretical DLVO profile from the measured force–distance profiles.

Below the pI, the difference between the measured and the theoretical (DLVO) force–distance profile, although small, was significant, suggesting that weak steric interactions were involved. At such low pH values, proteins are known to denature,[51] or form a molten globular state.[52] When denatured or even partially denatured, the gyration radius of a protein is increased. This denaturation of the proteins could explain the observed steric interactions. For this case, at large normalized forces, a thickness of about 8 nm is equal to about two adsorbed hydrated HSA layers (one flat-on monolayer on each mica surface; see Figure 5).

Table 1. Summary of HSA–HSA Interaction Results in 10^{-2} M KCl

pH	theoretical Debye decay length (nm)	measured decay length (nm)	thickness of adsorbed layer (nm)
2	2.2	5.6	4.0
4.8 (pI)	3.0	21.6	10.2
9	3.0	3.7	4.0

Above the pI (Figure 5, filled triangles), the force–distance profile showed a decay length in agreement with DLVO theory (3 nm). The thickness of each of the adsorbed layers was 4.0 nm, which suggests that the hydrated molecules were lying side on at the interface in their native state.

At the pI, however, steric forces were significant. The difference between the results at the pI and at other pH values is interesting. The behavior at the pI was confirmed by a measurement of the interactions between HSA and a bare mica surface (not shown) in which a long-range steric repulsion was also measured. The long range-force suggests that a fraction of HSA molecules were partially unfolded. The thickness of each of the adsorbed layers was much larger than that measured above or below the pI.

Interactions between HSA layers have also been studied by Blomberg et al.[39] However, their protocol was some-

(51) Pincet, F.; Perez, E.; Belfort, G. Do denatured proteins behave like polymers? *Macromolecules* **1994**, *27*, (12) 3424–3425.

(52) Alonso, D. O. V.; Dill, K. A.; Stigter, D. The three states of globular proteins: Acid denaturation *Biopolymers* **1991**, *31*, 1631–1649.

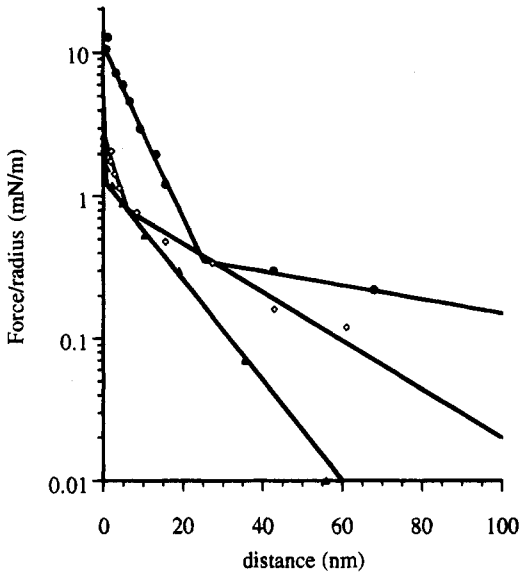

Figure 6. Normalized force versus separation distance between a deposited film of cellulose acetate and an adsorbed human serum albumin protein layer in a 10^{-2} M KCl solution at pH 2 (filled circles), pH 4.8 (open diamonds), and pH 9 (filled triangles). The full lines represent the curves obtained with the values given in Table 2. The distance was that between the precompacted cellulose acetate film and a compressed layer of human serum albumin. Only decompression is shown.

what different from that used in this study. They conducted their adsorption and SFA measurements at pH 5.5 and 10^{-3} M NaCl, while we varied pH values (2, 4.8, and 9) and used 10^{-2} M KCl. All our measurements were with 5×10^{-3} mg of HSA/mL, while they varied HSA concentration (0.001, 0.01, and 1 mg of HSA/mL). Another important difference, however, is that they conducted their direct force measurements *in* the protein solution and varied the protein concentration while in our experiments the protein solution was replaced with a pure KCl solution (with the same ionic strength as the protein solution) at different pH values. This may explain why the results presented here are slightly different from theirs. As mentioned above, we obtained an adsorbed layer thickness of 4.0 nm, while they report 2.3 nm for the thickness of a layer at the pI at 10^{-3} mg of HSA/mL. They explain their result by suggesting that the adsorbed protein has been compressed below its free solution dimension.

Forces between Protein Layers and a CA Film. For the two proteins, HSA and RNase A, only repulsive forces were measured. For HSA, the absence of attraction was confirmed by a measurement of the adsorption isotherms (not shown) at 20 ± 0.5 °C. From UV absorption spectroscopy of the solution, no detectable adsorption was measured between HSA and the CA membranes over several hours. To compare the results at the different pH values, three parameters were used to characterize the repulsion: in the semilog plots the data followed two lines of different slopes; and the force at which the change in slope occurred is called the "force at the knee".

The normalized force between adsorbed HSA and the CA film is given in Figure 6 and Table 2. We found that the measured decay lengths decreased with increasing pH values. Similar behavior was observed for the interaction between RNase A and a CA film (Figure 7 and Table 3). The main difference between the force–distance results for the two proteins is that, at high pH values (9.2 and 11), the force between RNase A and a CA film was dominated by short-range steric interactions

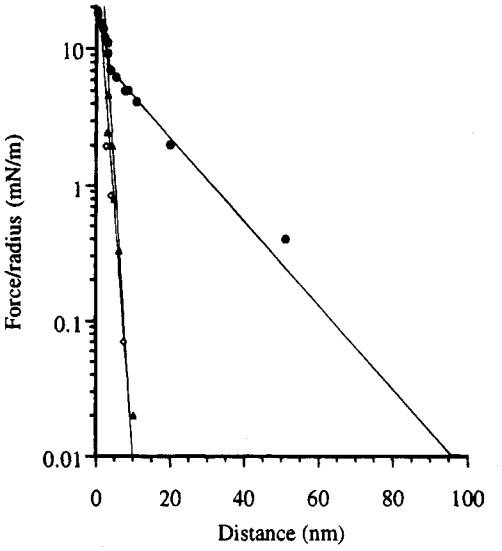

Figure 7. Normalized force versus separation distance between a deposited film of cellulose acetate and an adsorbed ribonuclease A protein layer in a 10^{-2} M KCl solution at pH 5 (filled circles), pH 9.2 (open diamonds), and pH 11 (filled triangles). The full lines are from fits to the data with the values given in Table 3. The distance was that between the precompacted cellulose acetate film and a compressed layer of ribonuclease A. Only decompression is shown.

Table 2. Summary of HSA–CA Interaction Results in 10^{-2} M KCl

pH	force at the knee (mN/m)	decay length (nm)	
		short-range	long-range
2	0.5	7.4	60
4.8 (pI of HSA/CA)	1	4.7	21
9	1.2	0.6	12

Table 3. Summary of RNase A–CA Interaction Results in 10^{-2} M KCl

pH	force at the knee (mN/m)	decay length (nm)	
		short-range	long-range
4.8 (pI of CA)	7	3.9	14
9.2 (pI of RNase A)	<0.01	1.2	
11	<0.01	1.1	

Table 4. Type of Interactions Observed for Each Experiment, at, above, and Below the Isoelectric pH of the Proteins[a]

	pH < pI		pH = pI		pH > pI	
	e^-	st	e^-	st	e^-	st
CA–mica	0	0	0	0	+	0
HSA–HSA	+	+	0	+	+	0
HSA–CA	0	+	0	+	+(?)	+
RNase A–CA	0	+	0	0	0	0

[a] e^- represents electrostatic interactions. st represents long-range steric interactions. + means that the indicated interaction was involved in the experiment. 0 means that the indicated interaction was not involved in the experiment.

involving one layer of native RNase. For HSA–CA interactions, long-range steric forces were always observed.

Discussion

Only repulsive forces were observed between CA films and protein layers. These repulsive forces are likely due to steric interactions. For each experiment, the kind of force involved is shown in Table 4. The CA–mica results indicated that the CA membrane was stable at all pH values and that polymer chains did not extend from its

surface into the solution. Therefore, any steric forces have to be attributed to the proteins and not to the CA film. This point is crucial, as steric interactions were then caused by the denatured protein molecules.

At low pH, for the HSA–HSA, HSA–CA, and RNase A–CA experiments, steric interactions were observed, indicating that at least some of the proteins were denatured. No steric forces and thus no denaturation was observed when forces between two adsorbed RNase A layers were measured at the same low pH.[38] This implies that the CA film caused RNase A denaturation during the experimental process. It should also be noted that, even without the CA film, some HSA molecules were denatured well below the pI.[51] Unfolding of the proteins could have been enhanced by the compression–decompression of the two mica-covered surfaces. It may even have been possible that a few protein molecules could have anchored into the surface pores of the membrane. If the fraction of protein molecules involved in bridging was low, the expected attraction during separation of the surfaces would have been too small to detect. This could explain why attractive forces were not observed for these measurements. Also, at these low pH values, proteins are known to denature.[53–56] Therefore, in a pressure-driven membrane process, as soon as the adsorbed proteins are exposed to low pH and fluid shear stresses, they denature and block the pores.

At high pH values, however, hardly any steric forces were measured for RNase A, suggesting that the proteins were not denatured. For HSA, the protein still denatured but less so than at lower pH values. Apparently, at these pH values and ionic strengths, the presence of a CA film did not significantly affect the protein structure. Therefore, the CA film did not interact with the protein during the force measurement in the same way as at low pH. Adsorption of the protein on CA was not observed, suggesting that significant membrane fouling would not be expected at these high pH values.

At the pI of the protein, the HSA–CA force–distance diagram showed long-range steric interactions while the RNase A–CA interactions were mainly short-range. Again these protein/protein measurements showed that HSA was less stable at the pI than RNase A.[38] This result is consistent with their respective adiabatic compressibility values (cf. above). So, in the case of HSA, membrane fouling is expected by denaturation. To summarize the results with HSA, RNase A, and CA, membrane fouling will most likely be due to protein denaturation and could be reduced by operating at high pH, provided that the membrane and protein are stable at this high pH. Also, denaturation is less likely to happen with hard proteins such as RNase A than with soft proteins such as HSA.[57,58]

Why did the observed electrostatic interactions not induce attractive forces? By considering the type of electrostatic charges on each material (Table 5), it appears that for all the pH values both surfaces had the same type of charge. Also, in the presence of CA membrane, HSA was much less stable than RNase A and tended to denature more easily. Thus, attraction was likely present for HSA, but because a net repulsive force was observed, steric interactions were dominant.

Table 5. Type of Charge on Each Material[a]

pH	HSA	CA	RNase A
2	+	+	NS
4.8	0	0	+
9.2	−	−	0
11	NS	−	

[a] The pI values for the HSA, CA, and RNase A are approximately 4.8, 4–5, and 9.2, respectively. Positively, negatively, and net neutrally charged surfaces are denoted by +, −, and 0, respectively. Doubly charged materials are strongly charged. The cases that were not studied are denoted by NS.

Conclusion

The main conclusions of this study are (i) at low pH values HSA and RNase A molecules are denatured (i.e. would induce membrane fouling); (ii) at high pH values, the proteins were less denatured than at lower pH values (i.e. would be less likely to foul); and (iii) HSA was more easily denatured and interacted more strongly with CA membranes than RNase A. Previous work has shown that (i) proteins were susceptible to denaturation at low pH values[52–56] and (ii) RNase A was more conformationaly stable than HSA during adsorption on polystyrene latex, i.e., HSA was denatured more easily at interfaces and was more sensitive to pH changes than RNase A.[59] It is also at the pI that more intense fouling occurs with hydrophobic membranes.[2,19] We believe that these results explain the observations of Fane et al.,[2] who obtained for a 0.1% BSA solution with no salt and with 0.2 M NaCl higher fluxes at pH values above the pI of BSA (at pH values of 10) [see their Figure 7]. Thus, these measurements provide the first molecular evidence that disruption of the protein tertiary structure could be responsible for the reduced permeation flows observed during membrane filtration and suggest that operating at high pH values away from the pI of the proteins will reduce such fouling. Also, we suggest that protein stability (i.e. as measured by the adiabatic compressibility) and membrane polymer composition are important factors in membrane fouling.

For a more complete understanding of the effect of protein adsorption on membrane filtration, force measurements with hydrophobic materials such as polysulfone and consideration of shear forces and their effect on protein stability would also have to be considered.

Appendix A

Validity of the Derjaguin Approximation during Deformation of the Glue and Compaction of the Cellulose Acetate (CA) Film in the Surface Forces Apparatus. After compaction, a likely geometry of the compacted CA film is shown in Figure 8. This configuration suggests that the measured force was that between two parallel surfaces in zone A (zone B gave negligible contributions because the uncompacted CA film was soft and the distances were large). The forces can then be reanalyzed by assuming this configuration: the area over which the surfaces are parallel can be calculated from the thickness of the uncompacted and compacted CA films and the radius of curvature of the surfaces. If this process is followed, the ensuing problem arises: the force–distance curves obtained in this way were not reproducible anymore, while, with the Derjaguin's approximation, they

(53) Goto, Y.; Fink, A. L. Phase diagram for acidic conformational states of apoxyoglobin *J. Mol. Biol.* **1990**, *214*, 803–805.
(54) Anderson, D. E.; Becktel, W. J.; Dahlquist, F. W. pH induced denaturation of proteins: A single salt bridge contributes 3–5 kcal/mol to the free energy of folding of T4 lysozyme *Biochemistry* **1990**, *29* (9), 2403–2408.
(55) Puett, D. The equilibrium unfolding parameters of horse and sperm whale myoglobin *J. Biol. Chem.* **1973**, *248* (13), 4623–4634.
(56) Creighton, T. E. *Proteins: Structures and Molecular Properties*, W. H. Freeman and Co.: New York, 1984.
(57) Kharakoz, D. P.; . Sarvazyan, A. P Hydrational and intrinsic compressibilities of globular proteins *Biopolymers* **1993**, *33*, 11–26.
(58) Gekko, K.; Yamagami, K. Flexibility of food proteins as revealed by compressibility *J. Agric. Food Chem.* **1991**, *39*, 57–62.
(59) Hesselink, F. Th. In *Adsorption from Solution at the Solid/Liquid Interface*; Parfitt, G. D., Rochester, C. H., Eds.; Academic Press, New York, 1983; Chapter 8.

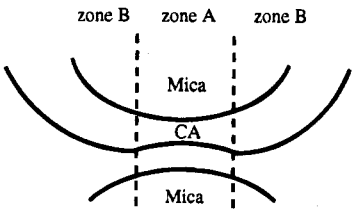

Figure 8. Hypothetical diagram of the compaction of cellulose acetate film in the SFA.

were highly reproducible over the whole set of experiments. This reproducibility cannot be fortuitous and a possible reason why Derjaguin's approximation remains valid is presented below.

The CA films were precompacted under large forces (i.e. >20 mN/m, which is larger than those shown in Figures 4–7). Under these conditions, the surfaces were substantially deformed: Attard and Parker[60] give the relation between the flattening of the surfaces, the force, and the elasticity of the surfaces [which was due to the *glue*: $E/(1-n^2) = 0.36\ 10^{-10}$ J m^{-3}, (Loubet, J. L., private communication), where E is Young's modulus and n is Poisson's ratio]. In our case, the surfaces were deformed by about 30 nm (due to the glue), and the geometries of the surfaces before, during and after compaction were as shown in Figure 9. Thus, for the surface area over which

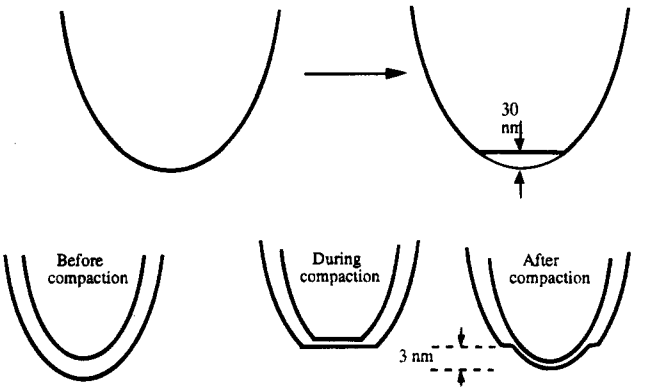

Figure 9. Surface deformation due to glue during compaction of the cellulose acetate film.

the forces interacted, the geometry remained crossed cylindrical, albeit with a thinner CA film than prior to compaction, and the Derjaguin's approximation remained valid.

Acknowledgment. We acknowledge the support of the U. S. Department of Energy, Basic Chemical Science Division (Grant No. DE-FG02–90ER14114). Bob L. Riley kindly supplied the cellulose acetate polymer. We thank Jeffrey A. Koehler and Brian Frank for discussions and Cheng Sheng Lee for measuring the RNase A adsorption kinetics shown in Figure 1.

LA9305280

(60) Attard, P.; Parker, J. L. Deformation and adhesion of elastic bodies in contact *Phys. Rev. A* **1992**, *46* (12), 7959–7971.